

Original article

# The explosive fracturing technique analysis for highly low permeable reservoirs using analytical, displacement discontinuity and finite difference coupled method

Mohammad Fatehi Marji<sup>1</sup>, Meysam Lak<sup>2\*</sup>, Manouchehr Sanei<sup>3</sup>

1- Professor, Department of Mining and Metallurgy, Yazd University, Yazd, Iran

2- PhD of Rock Mechanics, Department of Mining and Metallurgy, Yazd University, Yazd, Iran

3- Assistant Professor, Department of Mining and Metallurgy, Yazd University, Yazd, Iran

Received: 20 August 2023; Accepted: 22 October 2023

DOI: 10.22107/JPG.2023.412506.1208

## Keywords

Explosive rock fracturing,  
Unconventional reservoirs,  
Green's function,  
Displacement discontinuity  
method,  
Finite difference method,  
Radial cracks

## Abstract

Crack propagation in the low permeable reservoir rock as an explosive fracturing technique can be used to increase the permeability and productivity of unconventional reservoirs. This technique is the same as hydraulic fracturing but uses blast-induced shock waves and gas pressure to generate and propagate radial cracks around the wellbore in a particular reservoir. In this study, we want to simulate the explosion-induced crack initiation and propagation around a wellbore as a stimulation method of unconventional reservoirs using an analytical-numerical technique. Therefore, the dynamic crack initiation and propagation process of deep rock caused by the explosion is considered both analytically and numerically. The mechanical process of rock cracking under the action of an explosion stress wave is theoretically analyzed and simulated with a finite difference method. Then the coupling effect of explosion load in the form of shock wave and gas pressure is established numerically based on the two-dimensional explicit finite difference and displacement discontinuity methods, respectively. The analytical method involved the solution of the Lamé-Navier equation in elasto-dynamics based on the Green's function solution. The simulation procedure consists of coupling the explicit finite difference method with the displacement discontinuity method in the form of higher-order displacement discontinuities along the boundaries of the problem. All of the mentioned processes have been done in an oil field with a density of 2.5 gr/cm<sup>3</sup>, Poisson's ratio of 0.2, and elastic modulus of 20 GPa. The numerical results of this research show that shock waves are responsible for the initiation and propagation of radial cracks around the wellbore which in turn is filled with pressurized gas due to explosion. Then, these shock wave-induced radial cracks are propagating in the reservoir rock because of the explosive gas pressure inside them. This rock fracturing mechanism can help to improve the permeability and productivity of the highly low-permeable reservoirs in horizontal wells.

## 1. INTRODUCTION

Explosive fracturing can be used to increase the productivity of the reservoir's rock. The process is the same as that of hydraulic fracturing techniques but uses blasting to generate and propagate radial cracks around the wellbore in a particular reservoir. It is claimed that the

application of hydraulic fracturing in the reservoirs with unconnected fractures, may not be effective. Therefore, it makes the feasibility study of alternative methods interesting.

The explosive fracturing technique can be applied to initiate and propagate the radial fractures around a wellbore due to shock waves

\* Corresponding Author: meysamlak.ml@gmail.com

and a large amount of gas produced by the explosion. Previously, some different waterless fracturing methods and explosive-based stimulation techniques were studied [1–5]. The explosion-induced fractures may be used for stimulating the reservoir rocks and increasing the oil and gas productivity of these reservoirs which can be an interesting subject in petroleum geomechanics. The implementation of explosive fracturing techniques has already been investigated as a productive oil/gas method [6]. Also, several already available explosives have been suggested for a waterless fracturing treatment as an alternative [7]. The results from some field applications of the explosive fracturing in New Mexico, Oklahoma, and Texas oil fields were exhibited in [8]. Moreover, an analytical investigation of the explosive fracturing in the oil and gas wells was performed using mathematical methods [9]. Some non-aqueous fracturing techniques (such as liquid CO<sub>2</sub>, nitrogen fracturing, foams, LPG fracturing, and explosive fracturing) for reservoir stimulation were also investigated and compared as alternatives to hydraulic fracturing [10–12]. The methane deflagration fracturing technology is one of the non-aqueous fracturing techniques that have been recently investigated by some researchers [13,14]. Rogala et al. concluded that in non-aqueous fracturing technologies, application of the explosive fracturing provides the most cost-effective and environmentally friendly stimulation method [10]. Zhu et al. have studied improving reservoir permeability using electric pulse controllable shock wave [15]. Several studies were carried out on the initiation and propagation of the blast-induced radial cracks around the wellbore [16–18]. Sheng et al. proposed and solved flow behavior analysis of a complex-flow model for the explosive fracturing of a well in an unconventional reservoir [19]. Settgaest et al. developed a new computational model for predicting late-time gas-driven fracturing using propellants and high explosives [20]. Some previous research has been focused on the numerical modeling and fractal analysis of the radial shock wave and fracture propagation in petroleum reservoirs [21,22].

Fracture mechanics has been applied to a range of rock engineering problems, such as explosive fracturing, rock cutting, hydraulic fracturing, and rock slope stability [23–28]. Fracture mechanics is mainly applied in the

domain of the principles of Linear Elastic Fracture Mechanics (LEFM) and used in rock fracture mechanics as a computational theory [29–31]. Investigation of the mechanical behavior of rocks affected by high explosion loads is difficult and costly. It is usually studied exclusively by instrumentation and experimental works. Besides, the explosion-induced fractures in rock propagate very quickly and the experimental work needs to take a lot of time and cost for the investigation of dynamic fracture mechanics in rocks. Therefore, dynamic rock fracture mechanisms have been studied by many researchers using experimental and sophisticated numerical methods [32,33]. Omidimanesh et al., have focused on the fracture propagation properties around an oil well [34]. Many other studies are focused on the effects of in-situ stresses and load density on the rock fracturing process to investigate crack initiation and propagation due to blasting [5,35]. Moreover, variations of the displacement discontinuity method considering the elastic and poroelastic media and the discrete element method were used by many investigators in geomechanics [23,36–39]. They numerically modeled the mechanism of crack propagation of hydraulic fractures from a wellbore. However, long cracks formed by pre-splitting blasting in deep holes have a significant impact on the control of subsequent excavation disturbances. The investigation of the dynamic evolution process of these long cracks which are usually in the form of radial cracks around the boreholes is practically beneficial for the design of deep hole blasting too.

Numerous domestic and international investigations carried out to explain the mechanism of the rock cracking and fracturing process around the wellbores due to explosion. They considered the effects of the initial explosion stress wave and the foredooming explosion gas pressure on the rock mass failure and fracturing around the wellbores [4,33,40–43]. The crack length and area decrease as the initial stress increases. Many researchers [44,45] have found that cracks mainly propagate in the direction of high principal stress. They also claimed that both the stress wave distribution around the borehole and the effect of blasting gas affected crack initiation and early propagation [46].

It should be considered that the widely accepted traditional blasting of deep hole theory currently describes the blasting process by the combined action of explosive stress wave and

pressurized explosive gas. This theory explains that the stress wave generated by each blast hole first generates some initial micro-cracks and about 6 to 12 radial cracks around the blast hole which expand further under the interference of the stress wave. Then the pressurized gas penetrates the crack surface under the static pressure of the explosion [47]. On the other hand, the induced unloading effects due to the surrounding rock cracking process under the original rock stress field complicate the dynamic crack propagation mechanism in the blasting operation. This concept emphasizes the significance of the simultaneous effects of explosion stress wave and explosion-generated gas pressure in the process of crack formation around a borehole due to blasting. This concept shows the mechanism of radial crack propagation due to borehole explosion in a rock mass is very complicated and states that the instantaneous characteristics of rock blasting (by explosives) make determining the dynamic cracking process difficult [48].

In this study, to stimulate the host rock of the unconventional reservoirs, the explosion-induced crack initiation and propagation around a wellbore have been simulated using an analytical-numerical technique. Thus, the general radial crack initiation and propagation around a wellbore in an Iranian oil field due to rock blasting is considered. As shown in the literature, most of the previous studies have been focused on hydraulic fracturing as a stimulation method. It should be noted that some researchers studied the rock fracturing methods using explosion, but they often focused only on the crack propagation due to gas pressure. The presented study has modeled crack propagation in rock reservoirs using both phases of explosion, shock wave, and gas pressure. The problem is treated analytically and numerically based on the concept presented in the previous paragraph. The numerical simulation procedure involves a coupled finite difference-boundary element approach. Moreover, the entire process of rock fracture, including crack initiation and propagation, is considered.

## 2. Mathematical Formulations

In this study, firstly the analytical solution for the crack initiation due to shock wave around the wellbore is considered to verify the numerical results predicted by the explicit finite difference code, FLAC2D. Then, two numerical schemes, namely the Finite Difference Method (FDM) and

Indirect Boundary Element Method (IBEM) are used to model the explosion-induced radial cracks propagation around a wellbore. This numerical simulation scheme consists of two stages, firstly, modeling of cracks initiation because of shock wave propagation by considering the FDM method and, secondly, modeling of the radial crack propagation because of gas expansion considering the BEM method. The proposed method can completely model crack initiation and propagation process due to explosion. The process has been considered in both shock wave propagation and gas expansion phases. In this case, can be analytically and numerically modeled a stimulation technique for the unconventional reservoirs.

### 2.1. Analytical Solution for Shock-wave Crack Initiation

Rock blasting impacts on the rock mass is a fundamental topic in rock mechanics. Rock blasting is a dynamic phenomenon that consists of two steps, namely shock wave propagation and gas expansion. The shock wave propagation step can be considered to analyze the explosion-induced wave in the rock. The analytical solution was developed for two-dimensional in an elastic, isotropic, homogenous, and continuum media by [33].

In this study, the mentioned analytical solution is used to initiate the crack and then compare its results with the FDM method which will be explained in the next section. The analytical solution is presented as follows:

The Navier's equations of motion were used as governing equations [49]. Green's function was calculated to present the time-dependent explosion loading behavior. The general elastodynamic Green's function was presented in terms of displacements. Moreover, the strain and stress are expressed based on the theory of elasticity by considering the analytical solution of displacement.

#### 2.1.1. Governing equations for elasto-dynamic behavior

The general form of elastodynamic equation of motion is:

$$\sigma_{ij,j} + \rho f_i = \rho \ddot{u}_i \quad (1)$$

The motion of an isotropic, homogeneous elastic body is presented by Navier's equation as:

$$\begin{aligned}
& (\lambda' + \mu)u_{i,jj} + \mu u_{i,jj} + \rho f_i \\
& = \rho \ddot{u}_i (\lambda' + \mu) \nabla (\nabla \cdot u) + \mu \nabla^2 u + f \\
& = \rho \partial^2 u / \partial t^2
\end{aligned} \quad (2)$$

where, the constant  $\lambda'$  is:

$$\lambda' = \begin{cases} \lambda & \text{Plane strain} \\ \frac{2\lambda\mu}{(\lambda + 2\mu)} & \text{Plane stress} \end{cases} \quad (3)$$

where  $\lambda$  is Lamé constant and  $\mu$  is the shear modulus.

### 2.1.2. Presentation of the displacement of the Green's function

The Navier's equation can present as follows [50]:

$$\begin{aligned}
& \rho M^P \left( c_p^2 \nabla^2 A^P - \frac{\partial^2 A^P}{\partial t^2} \right) \\
& + \rho M^S \left( c_s^2 \nabla^2 A^S - \frac{\partial^2 A^S}{\partial t^2} \right) + f = 0
\end{aligned} \quad (4)$$

Based on the Helmholtz theory, Poisson's equation, namely  $\nabla^2 \varphi = q(x)$  has the general solution as:

$$\varphi = - \int_{\text{all space}} \frac{q(x')}{4\pi|x-x'|} dv' \quad (5)$$

By considering a variety of steps presented in the [33] article, the displacement of the Green's function can drive the following relationship:

$$\begin{aligned}
& u_j(x, t) \\
& = -\delta_{jk} \nabla^2 \left( \frac{P_k(t)}{4\pi\rho r} \right) \\
& + \frac{\partial^2}{\partial x_j \partial x_k} \left( \frac{P_k \left( t - \frac{r}{c_p} \right)}{4\pi\rho r} \right) \\
& + \left( \delta_{jk} \nabla^2 - \frac{\partial^2}{\partial x_j \partial x_k} \right) \left( \frac{P_k \left( t - \frac{r}{c_s} \right)}{4\pi\rho r} \right)
\end{aligned} \quad (6)$$

where  $\delta_{jk}$  is the Kronecker delta.

### 2.1.3. Functions for evaluating strain and stress

By applying the external loading, elastic rock media will be deformed. The deformation is presented by displacement and strain. After defining the displacement function, the strain can be obtained using the theory of elasticity, as follows [51,52]:

$$\varepsilon_{ji} = \frac{1}{2} (u_{j,i} + u_{i,j}) \quad (7)$$

Then, by considering the above equation, the strain can be expressed as the following relationship:

$$\begin{aligned}
\varepsilon_{jl} & = \frac{3\delta_{jk}(\gamma_l + \gamma_j) - 18\gamma_j\gamma_k\gamma_l}{4\pi\rho r^4} p_0 \xi Z_1 \\
& + \frac{6\gamma_j\gamma_k\gamma_l - \delta_{jk}(\gamma_l + \gamma_j)}{4\pi\rho r^3} p_0 \xi Z_2 \\
& + \frac{-\gamma_j\gamma_k\gamma_l}{2\pi\rho c_p^2 r^2} p_0 \xi \left[ \exp\left(-\alpha\left(t - \frac{r}{c_p}\right)\right) \right. \\
& \left. - \exp\left(-\beta\left(t - \frac{r}{c_p}\right)\right) \right] \\
& + \frac{\gamma_j\gamma_k\gamma_l}{2\pi\rho c_p^3 r} p_0 \xi \left[ \alpha \exp\left(-\alpha\left(t - \frac{r}{c_p}\right)\right) \right. \\
& \left. - \beta \exp\left(-\beta\left(t - \frac{r}{c_p}\right)\right) \right] \\
& + \frac{2\gamma_j\gamma_k\gamma_l - \delta_{jk}(\gamma_l + \gamma_j)}{4\pi\rho c_s^2 r^2} p_0 \xi \left[ \exp\left(-\alpha\left(t - \frac{r}{c_s}\right)\right) \right. \\
& \left. - \exp\left(-\beta\left(t - \frac{r}{c_s}\right)\right) \right] \\
& + \frac{\delta_{jk}(\gamma_l + \gamma_j) - 2\gamma_j\gamma_k\gamma_l}{4\pi\rho c_s^3 r} p_0 \xi \left[ \alpha \exp\left(-\alpha\left(t - \frac{r}{c_s}\right)\right) \right. \\
& \left. - \beta \exp\left(-\beta\left(t - \frac{r}{c_s}\right)\right) \right]
\end{aligned} \quad (8)$$

By using the general form of stress-strain relationship as defined as follows [53–55]:

$$\sigma_{jl} = \lambda \varepsilon_{mm} \delta_{jl} + 2\mu \varepsilon_{jl} \quad (9)$$

We can express the stress of each particle as follows:

$$\begin{aligned}
\sigma_{ij} & = \lambda \delta_{jl} \left\{ \frac{3\delta_{mk} - 9\gamma_m\gamma_k}{4\pi\rho r^4} \gamma_m p_0 \xi Z_1 + \right. \\
& \left. \frac{3\gamma_m\gamma_k - \delta_{mk}}{4\pi\rho r^3} \gamma_m p_0 \xi Z_2 + \right. \\
& \left. \frac{-\gamma_m\gamma_k\gamma_m}{4\pi\rho c_p^2 r^2} p_0 \xi \left[ \exp\left(-\alpha\left(t - \frac{r}{c_p}\right)\right) \right. \right. \\
& \left. \left. \exp\left(-\beta\left(t - \frac{r}{c_p}\right)\right) \right] \right\} + \\
& \left. \frac{\gamma_m\gamma_k\gamma_m}{4\pi\rho c_p^3 r} p_0 \xi \left[ \alpha \exp\left(-\alpha\left(t - \frac{r}{c_p}\right)\right) \right. \right.
\end{aligned} \quad (10)$$

$$\begin{aligned} & \beta \exp\left(-\beta\left(t - \frac{r}{c_p}\right)\right) \Bigg] + \\ & \frac{\gamma_m \gamma_k - \delta_{mk}}{4\pi \rho c_s^2 r^3} \gamma_m p_0 \xi \left[ \exp\left(-\alpha\left(t - \frac{r}{c_s}\right)\right) - \exp\left(-\beta\left(t - \frac{r}{c_s}\right)\right) \right] + \\ & \frac{\delta_{mk} - \gamma_m \gamma_k}{4\pi \rho c_s^3 r} \gamma_m p_0 \xi \left[ \alpha \exp\left(-\alpha\left(t - \frac{r}{c_s}\right)\right) - \beta \exp\left(-\beta\left(t - \frac{r}{c_s}\right)\right) \right] \Bigg] + \\ & 2\mu \left\{ \frac{3\delta_{jk}(\gamma_l + \gamma_j) - 18\gamma_j \gamma_k \gamma_l}{4\pi \rho r^4} p_0 \xi z_1 + \frac{6\gamma_j \gamma_k \gamma_l - \delta_{jk}(\gamma_l + \gamma_j)}{4\pi \rho r^3} p_0 \xi z_2 + \frac{-\gamma_j \gamma_k \gamma_l}{2\pi \rho c_p^2 r^2} p_0 \xi \left[ \exp\left(-\alpha\left(t - \frac{r}{c_p}\right)\right) - \exp\left(-\beta\left(t - \frac{r}{c_p}\right)\right) \right] + \frac{\gamma_j \gamma_k \gamma_l}{2\pi \rho c_p^3 r} p_0 \xi \left[ \alpha \exp\left(-\alpha\left(t - \frac{r}{c_p}\right)\right) - \beta \exp\left(-\beta\left(t - \frac{r}{c_p}\right)\right) \right] + \frac{2\gamma_j \gamma_k \gamma_l - \delta_{jk}(\gamma_l + \gamma_j)}{4\pi \rho c_s^2 r^3} p_0 \xi \left[ \exp\left(-\alpha\left(t - \frac{r}{c_s}\right)\right) - \exp\left(-\beta\left(t - \frac{r}{c_s}\right)\right) \right] + \frac{\delta_{jk}(\gamma_l + \gamma_j) - 2\gamma_j \gamma_k \gamma_l}{4\pi \rho c_s^3 r} p_0 \xi \left[ \alpha \exp\left(-\alpha\left(t - \frac{r}{c_s}\right)\right) - \beta \exp\left(-\beta\left(t - \frac{r}{c_s}\right)\right) \right] \right\} \end{aligned}$$

**2.1.4. Analytical solution of the problem**

The problem is a two-dimensional blast hole in an elastic, isotropic, homogenous, and continuum medium whose elastic properties of rock mass and other features are similar to the article [56].

To present the displacement, strain, and stress around a typical blast wellbore, the equations that have been presented above, are considered. The seismic source in the blast wellbore is a time-dependent pressure function, as shown in Figure 1.

The displacement is expressed against distance from the blast hole  $r$  in which its variation for a constant time is present in Figure 2. As can be seen, there are two peaks in variations of displacement versus distance from the blast hole ( $r$ ). These peaks are relevant to the near-field

and far-field of the presented Green's function (Equation 6).

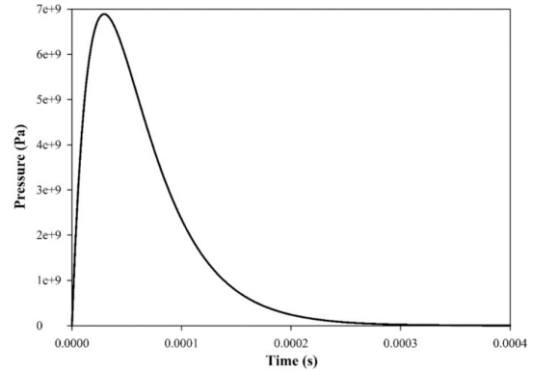


**Fig. 1.** An applied pressure pulse waveform for blast wellbore

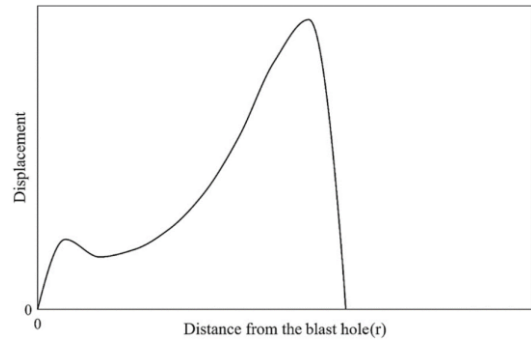


**Fig. 2.** Variations of displacement versus distance from blast hole ( $r$ )

Figure 3 indicates the displacement variations versus distance from the blast-wellbore ( $r$ ) for several constant times (shorter times). It is presented that as time passes, the near-field effects decrease and the far-field effects become governed.

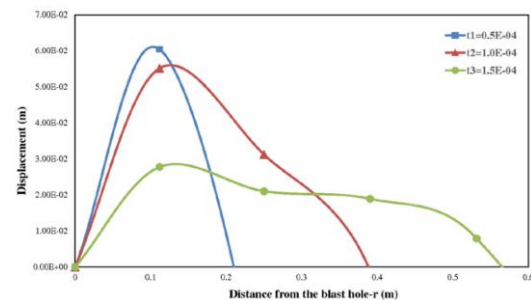


**Fig. 3.** Variations of displacement versus distance from blast wellbore

The blast hole problem above has been modeled using the analytical solution and the

numerical simulation which will be expressed in the next section. The results of them are calculated and the results are compared as indicated in Figure 4.

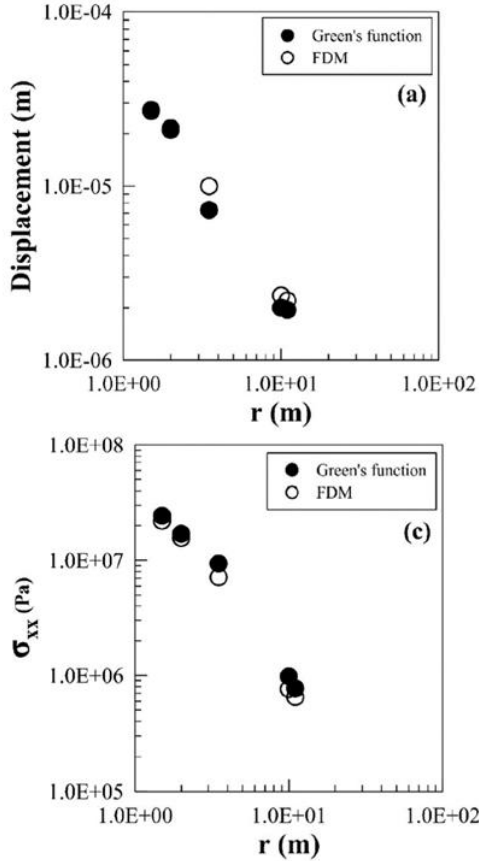


Fig. 4. Comparison of displacement and stress parameters computed from Green's analytical solution and FDM numerical modelling

### 2.2. Finite Difference Formulations

The finite difference is approximation of derivatives which plays a central role in the numerical solution of governing partial differential equations (GPDE) in boundary value problems (BVPs). The mathematical expression of finite difference method (FDM) can be expressed in the form of  $f(x + a_2) - f(x + a_1)$ . If a finite difference is divided by the differential increment  $\Delta a = (a_{k+1} - a_k)$ ,  $k = 1, 2, \dots, n$ , one may get a difference quotient [57].

There are generally three basic types of FDM expressions i.e., forward, central, and backward finite differences (as shown in Figure 5) [58].

Forward difference method is presented as:

$$\Delta[f](x) = f(x + \Delta a) - f(x) \quad (11)$$

where  $f$  is a function of BVP.

Central difference method is expressed by:

$$\Delta[f](x) = f\left(x + \frac{\Delta a}{2}\right) - f\left(x - \frac{\Delta a}{2}\right) \quad (12)$$

Backward difference method is introduced as:

$$\Delta[f](x) = f(x) - f(x - \Delta a) \quad (13)$$

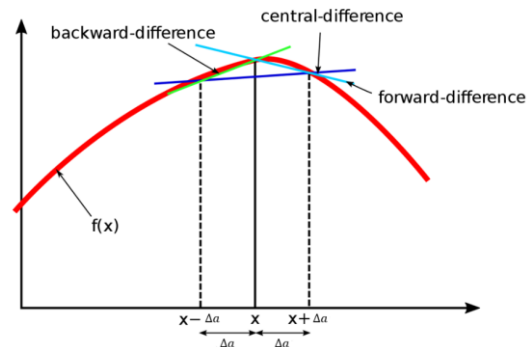


Fig. 5. Three types of finite differences, Forward, Central, and Backward difference method

The solution of solid-body, heat-transfer, or fluid-flow problems in FLAC invokes the equations of motion and constitutive relations, Fourier's law for conductive heat transfer, and Darcy's Law for fluid flow in a porous solid, as well as boundary conditions. Newton's law of motion for the mass-spring system is:

$$m \frac{d\dot{u}}{dt} = F \quad (14)$$

When several forces act on the mass, Equation 14 also expresses the static equilibrium condition when the acceleration tends to zero (i.e.,  $\Sigma F = 0$ , where the summation is over all acting forces). This property of the law of motion is exploited in FLAC when solving "static" problems. Note that the conservation laws (of momentum and energy) are implied by Equation 14, since they may be derived from it (and Newton's other two laws). In a continuous solid body, Equation 14 is generalized as:

$$\rho \frac{\partial \dot{u}_i}{\partial t} = \frac{\partial \sigma_{ij}}{\partial x_j} + \rho g_i \quad (15)$$

where  $\rho$  = mass density;

$t$  = time;

$x_i$  = components of coordinate vector;

$g_i$  = components of gravitational acceleration (body forces); and  
 $\sigma_{ij}$  = components of stress tensor.

**2.3. Indirect Boundary Element Method Formulation**

In this study, the indirect boundary element method using higher order displacement discontinuities along the crack elements is used to numerically simulate the crack propagation in a rock mass. The displacement discontinuity method is based on analytical solutions to the Kelvin problem along the line crack. The method computes the crack opening and crack sliding displacements in the form of normal and shear discontinuities along the surface of a crack element. The method builds a discrete approximation of the displacement discontinuity function along a crack [59]. The general distribution of the displacement discontinuity function  $u(ε)$  is shown in Figure 6. For the constant element displacement discontinuity along the crack element of length  $2a$ , the function  $u(ε)$  has the constant shear and normal components,  $D_x$  and  $D_y$  in the interval  $(-a, +a)$  [60].

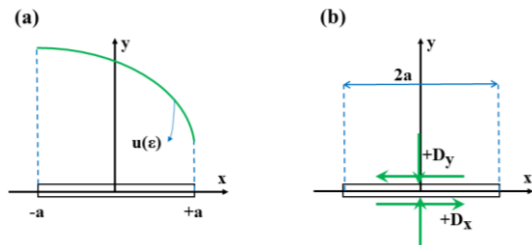


**Fig. 6.** a) A displacement discontinuity element and distribution function,  $u(ε)$ , b) displacement discontinuity components for a constant element of length  $2a$

The displacement discontinuity distribution can be described as a function of  $D_j = (D_x, D_y)$ , from the negative side of the element to the positive one. Therefore, the  $D_j$  function is defined as:

$$D_j = u_j(x, 0^-) - u_j(x, 0^+), \quad j = x, y \tag{16}$$

The variation of the quadratic shape function of the displacement discontinuities over a straight crack line is indicated in Figure 7.

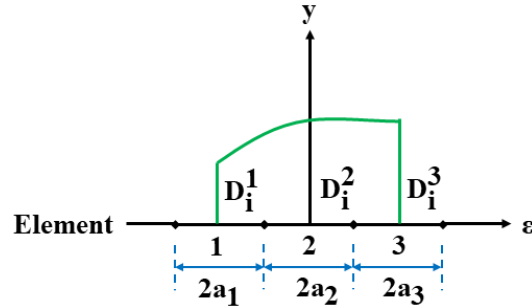


**Fig. 7.** Quadratic variation of displacement discontinuity over a line crack element (Shou and Crouch, 1995)

The quadratic shape function of the displacement discontinuities over a line crack is [61]:

$$D_j(ε) = N_1(ε)D_j^1 + N_2(ε)D_j^2 + N_3(ε)D_j^3 \tag{17}$$

where  $D_j^1, D_j^2,$  and  $D_j^3$  are the quadratic nodal displacement discontinuities for the nodes 1, 2, and 3, respectively. The shape function of  $N_1(ε), N_2(ε),$  and  $N_3(ε)$  for  $a_1 = a_2 = a_3,$  are:

$$\begin{aligned} N_1(ε) &= ε(ε - 2a_1) / 8a_1^2 \\ N_2(ε) &= -(ε^2 - 4a_1^2) / 4a_1^2 \\ N_3(ε) &= ε(ε - 2a_1) / 8a_1^2 \end{aligned} \tag{18}$$

The displacement discontinuity method which is the displacement version of the indirect boundary element method is modified for using the higher order displacement discontinuity elements and the special crack tip elements [24,31,62,63]. The quadratic element displacement discontinuity element is implemented in a two-dimensional code for crack analysis (TDDQCR).

The crack tips are considered to be the singular points due to the high-stress concentration at these points. Therefore, the stress and displacement fields near the crack tips should be treated specifically using some special crack tip elements [26,60]. The special crack tip elements are implemented in TDDQCR code as shown in Figure 8. The displacement discontinuities for a crack element are estimated as:

$$D_x(\varepsilon) = D_x(a) \left(\frac{\varepsilon}{a}\right)^{\frac{1}{2}} \tag{19}$$

$$D_y(\varepsilon) = D_y(a) \left(\frac{\varepsilon}{a}\right)^{\frac{1}{2}}$$

where  $\varepsilon$  is the distance from the crack tip and  $D_x(a)$  and  $D_y(a)$  are the opening and sliding components of the displacement discontinuities at the center of the special crack tip element.

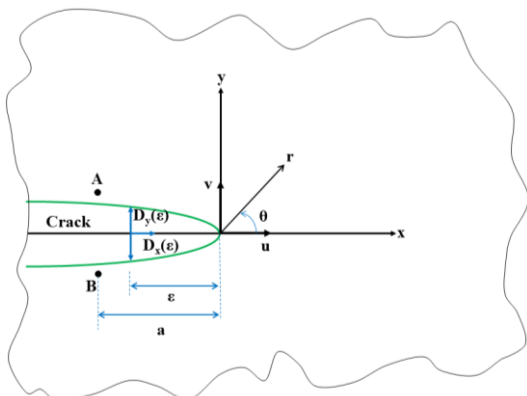


**Fig. 8.** Characteristics of a special crack tip element for shear and normal displacement discontinuity components  $D_x(\varepsilon)$  and  $D_y(\varepsilon)$ , respectively

### 3. Numerical Modelling

#### 3.1. Finite Difference Modeling (FDM)

The rock mass around the blast hole can be considered as a continuum therefore a continuum modeling approach can be used to solve the problem of crack initiation around a blasthole. In this research, the finite difference method (FDM) is used to simulate the process of radial crack initiation around a blast hole in an elastic rock medium. At the initial stage, the induced shock waves due to the explosion are considered to play the main role. Then the quasi-static radial crack propagation is modeled by indirect boundary element method to be explained in the next section.

In this study, the crack initiation process because of explosion in a wellbore is modeled based on the finite difference method using the two-dimensional Fast Lagrangian Analysis of Continua [64]. The simulation of the dynamic processes for blasting of a hole in an infinite rock mass is performed in FLAC2D based on the

specified dynamic boundary conditions [64]. These dynamic conditions are satisfied using absorbing boundaries which involves dashpots attached independently to the normal and shear directions along the problem boundaries [65]. The boundary tractions,  $t_i$  can be expressed as:

$$t_i = -\rho C_i v_i, \quad i = n, s \tag{20}$$

where  $v_n$  and  $v_s$  are the normal and shear components of the velocity at the boundary,  $\rho$  is the mass density and  $C_n$  and  $C_s$  are the primary (P) and secondary (S) wave velocities [64,66].

The viscous boundaries around the numerical models produce infinite propagation and absorption of waves without returning to the computing medium. The fracturing process in rock blasting by explosives is highly interesting in rock engineering applications but it is very complicated to be modeled numerically by the existing numerical methods. It is well established that the explosion can initiate and propagate radial cracks in the reservoir rock around a wellbore. It is also found that there are two main stages of crack initiation and propagation around the wellbore namely shock wave propagation and gas pressure expansion. At first, blast-induced shock waves propagate and can initiate radial cracks around the wellbore, it means that after the explosion the shock waves produced firstly and propagate around the blast hole producing radial cracks of reasonable lengths, and a highly pressurized gas of considerable volume is produced due to detonation of explosive materials which is responsible to extend the radial cracks and enhance their propagation into the rock mass around the wellbore. In this study, it is tries to couple both mentioned stages numerically to simulate the radial cracks initiation and propagation due to rock explosion. Therefore, an explosion is numerically modeled in a wellbore with a diameter of 0.2 m in an Iranian oil field. Figure 9 illustrates the geometrical characteristics and the far field boundary conditions for simulating the explosion effects around a wellbore.

The blast hole problem shown in Figure 9 is considered a two-dimensional problem and the rock mass is considered to be homogenous, continuous, isotropic, and of linear elastic behavior. The explosive charge within the blast hole constitutes the explosion source and the explosive characteristics and the far-field stress conditions are given in Table 1 [67].

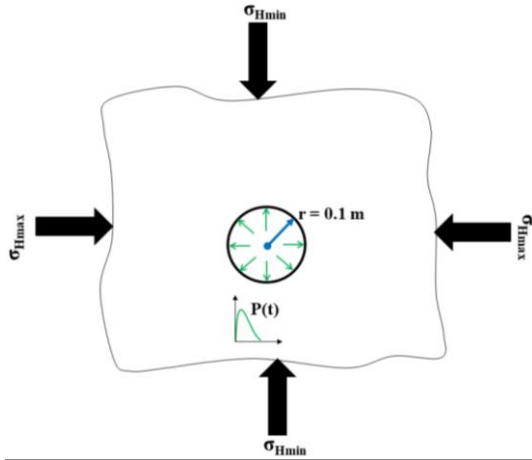


**Fig. 9.** Schematics of explosion stimulation model in FLAC 2D

**Table 1.** Characteristics of the studied area [68]

Properties	Values
Depth (m)	4014.5
Rock density (gr/cm <sup>3</sup> )	2.5
Poisson's ratio	0.2
Elastic modulus (GPa)	20
Uniaxial compressive strength (MPa)	20
Cohesion (MPa)	14.3
Friction angle (°)	46
σ <sub>Hmax</sub> (MPa)	92.5
σ <sub>Hmin</sub> (MPa)	82.2
Explosive density (gr/cm <sup>3</sup> )	1.2
Velocity Of Detonation-VOD (m/s)	4500

The explosion source is represented as a time-dependent pressure pulse or detonation pressure,  $P_d$ . The blasting pressure ( $P_d$ ) is the most important factor of the rock blasting mechanism and can be determined based on the explosive charge and rock mass properties. Many researchers worked on the subject for example [69,70] and proposed useful formulae for the detonation pressure. Jimeno et al., 1995 suggested a useful formula for detonation pressure based on the explosive density and the detonation velocity.

$$P_d = 432 \times 10^{-6} \times \rho_e \times \frac{V_d^2}{1 + (0.8\rho_e)} \quad (21)$$

where  $P_d$  is the detonation pressure in MPa, the explosive density is denoted as  $\rho_e$  in  $g/cm^3$  and  $V_d$  is the detonation velocity in  $m/s$  [70].

The pressure pulse  $P(t)$  is time-dependent and can be found based on the solution of a one-dimensional shock wave equation in the form of several useful functions [4,71,72]. The cavity

pressure due to explosion can be expressed in the form of two exponential functions [73].

$$P = P_0 N (\exp(-\alpha t) - \exp(-\beta t)) \quad (22)$$

where  $P$  is the explosion pressure,  $P_0$  is the maximum wall pressure and the variable  $N$  is a normalizing factor which normalizes the maximum pressure to  $P_0$  [74]. For the case study of this research, the variable  $N$  is estimated as 4. The frequency-dependent decay constants are given as the coefficients  $\alpha$  and  $\beta$  in Equation 20, the following relations are suggested by Brady and Brown, 2005 for the decay coefficients  $\alpha$  and  $\beta$  used in rock blasting.

$$\alpha = \omega / 4\sqrt{2} \quad (23)$$

$$\beta = \omega / 2\sqrt{2} \quad (24)$$

where,

$$\omega = \frac{2\sqrt{2}c_p}{3r_b} \quad (25)$$

$$c_p = \sqrt{\frac{K + \left(\frac{4\mu}{3}\right)}{\rho_r}} \quad (26)$$

In the above-mentioned equations,  $\rho_r$  is rock density  $r_b$  is borehole radius,  $c_p$  is the P-wave velocity in the rock media, and  $K$  and  $\mu$  are the bulk and shear moduli of the rock, respectively. Therefore, based on the characteristics listed in Table 1, the waveform generated by equation 15 is the same as that already shown in Figure 1.

The pressure pulse is numerically simulated in FLAC2D after the induced shock wave propagation around the wellbore in the continuum rock media. The symmetrically induced radial cracks (usually about 6 to 12 in number) are created around the wellbore. Considering the effects of shock wave propagation only and ignoring those of gas pressure, the plot of the plasticity zone around the wellbore is estimated by the finite difference model as shown in Figure 10a. However, the created fracture zone around the wellbore demonstrates 8 major radial cracks which are propagated in the rock mass ignoring the micro-cracks and immature cracks in the fractured area. The schematic configuration pattern of the eight major radial cracks is

reproduced in Figure 10b which can be used for further studies in the next section.

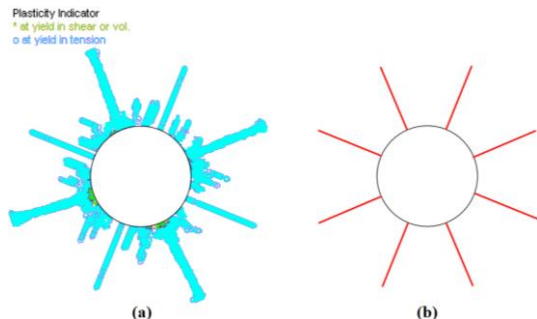


**Fig. 10.** a) Crack initiation around the wellbore,  
b) Sketch of the cracks pattern

### 3.2. Coupled dynamic FDM-DDM method

The mechanism of crack initiation and propagation around a blast hole in the form of radial cracks is considered to take place in two stages, the dynamic stage because of shock wave propagation and the quasi-static stage due to the pressurized gas expansion. Therefore, a dynamic finite difference method based on the central difference formulation (FLAC2D code) is adopted to model the first stage and a quasi-static higher-order displacement discontinuity method (TDDQCR code) is used to model the second stage.

#### 3.2.1. FDM modeling

In the first stage, dynamic finite difference modeling is performed to determine the radial crack initiation around the wellbore using FLAC software. Therefore, the problem stated in the previous section has been numerically simulated here. The input geomechanical properties and the other features of the explosion have also been considered similar to those given in Table 1. The dimensions of the FDM model are 10×10 meters and the borehole radius is 0.1 meter. Moreover, to set dynamic boundary conditions for the infinite rock medium, the quiet or absorbing boundaries were previously described have been utilized. The geometry of the geomechanical problem is the same as Figure 8 of the previous section (section 3.1). In the dynamic modeling stage of the problem using the finite difference approach, the far-field boundary conditions are the in-situ stresses and the characteristics of the shock wave pulse of explosive charges are considered as the input parameters. Then, the explicit central finite difference scheme implemented in the two-

dimensional Fast Lagrangian Analysis of Continua (FLAC2D) computer code [64] was used to solve the problem. The results of the dynamic modeling stage showed the radial crack's initiation patterns in the rock mass embedded in the wellbore. In the second stage, the initiated radial crack patterns of the first stage, the far-field stresses, and the gas expansion's properties of explosive materials are considered as input parameters. The results of this stage are exactly similar to those shown in Fig 10. The quasi-static boundary element modeling scheme implemented in the two-dimensional displacement discontinuity code using quadratic elements for crack analysis (TDDQCR) is used for the problem solution as explained in the next section.

#### 3.2.2. Quasi-static DDM modeling

The initiated radial crack patterns estimated by FDM and shown in Figure 10b are used in the second stage of the modeling process. In this stage, it is assumed that the driving force of the highly pressurized gas produced in the explosion stage is responsible for propagating the radial cracks around the blast hole. The indirect variation of displacement discontinuities along a line crack is modified for crack analysis and implemented in the TDDQCR code. The radial crack's pattern resulting from the dynamic crack initiation due to shock waves as given in Figure 10b is modeled by TDDQCR in which its formulations are briefly explained and, in this code, the theoretical background section of this research work. The results of this second stage of numerical simulation show that the pressurized explosion-induced gas plays a dominant role in further propagating the radial cracks within the rock mass which can be concluded that the propagation mechanism of the radial cracking of the rock around the wellbore is governed mainly by the pressurized gas driving because these gases formed in detonation and exert an exceedingly high pressure while flowing within the radial cracks. This induced gas pressure exerts outward pressure into the wellbore walls and radial cracks which is dependent upon the detonation pressure generated by the explosive and the explosive confinement in the wellbore [75]. In most cases, the gas pressure is usually of the order of 50% to 60% of the detonation pressure as given in Equation 19. Figure 11 shows the propagated radial cracks pattern after the gas expansion

modeling stage based on the above description and using the Table 1 properties. It means that the propagation mechanism of the radial crack's patterns due to the explosion of a rock media around a wellbore has been simulated and the resulting cracks pattern is shown in this figure.

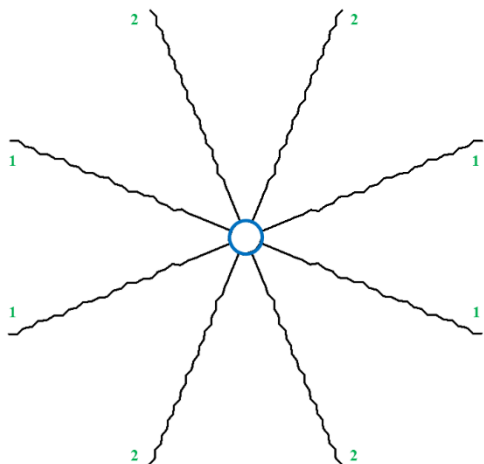


**Fig. 11.** Quasi-static modeling of propagation mechanism of explosion-induced radial cracks pattern around the wellbore

Figure 11 demonstrates the propagation mechanism of 8 radial cracks around the wellbore which eventually increase its productivity. The radial cracks are of two different lengths shown as 1 (which can extend to 141.44 cm in length) and 2 (which can extend to 136.4 cm in length). If the far-field stress is equal (a hydrostatic stress condition) then these two lengths are approximately equal and the radial cracks are symmetric. In the present case study, radial cracks 1 are propagated in the direction of the maximum horizontal stress ( $\sigma_{Hmax}$ ) and are longer compared to radial cracks 2 which propagated in the direction of minimum horizontal stress ( $\sigma_{hmin}$ ).

Moreover, inhomogeneity and anisotropy have significant effects on the radial crack length and their patterns. Pre-existing fractures in the host rock and some other failures in the host rock can also affect the radial crack propagation patterns due to explosion. However, these effective parameters are not relevant in the present study.

#### 4. Crack Propagation around a Horizontal Wellbore

The same procedure as explained above is done for crack propagation around the horizontal

wellbore. To perform this procedure, four hydraulic fracturing with equal lengths are numerically analyzed on each side of the horizontal wellbore. Because of the symmetry of the problem, a line of symmetry is considered as the boundary element, as shown in Figure 12.

The linear elastic fracture mechanics principles (LEFM) are adopted in TDDQCR code based on the Mode I and Mode II stress intensity factors and maximum tensile stress criterion to model the hydraulic fracturing process in the horizontal wellbore [23,33,39,67,76,77].

It is essential to mention that the first and second mode intensity factor namely  $K_I$  and  $K_{II}$ , namely the center slant crack problem are presented as follow [78]:

$$K_I = \sigma\sqrt{\pi b} \sin^2 \beta \quad \text{and} \tag{27}$$

$$K_{II} = \sigma\sqrt{\pi b} \sin \beta \cos \beta$$

The explosion gas pressure can be numerically modeled to produce a hydraulic fracturing process of a horizontal wellbore driven in an unconventional hydrocarbon reservoir. Figure 13 indicates the results obtained for different  $\beta$ . The numerical models are run for a maximum of 20 steps of crack propagation. The effect of  $\beta$  is analyzed on crack propagation. For instance, for  $\beta = 0.5$  the inner cracks have not propagated completely because of the impact of the outer crack.

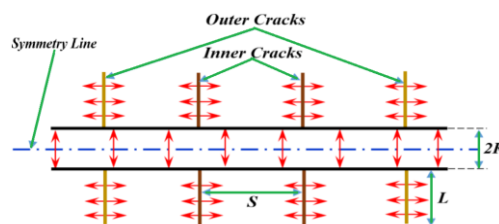


**Fig. 12.** A sketch of horizontal wellbore with hydraulic fracturing geometry

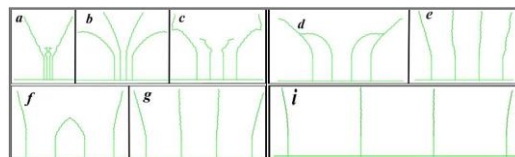


**Fig. 13.** Crack propagation for different value of  $\beta$ : a)  $\beta = 0.125$ , b)  $\beta = 0.25$ , c)  $\beta = 0.5$ , d)  $\beta = 0.75$ , e)  $\beta = 1.0$ , f)  $\beta = 1.25$ , g)  $\beta = 1.5$ , and i)  $\beta = 2.0$

## 5. Conclusion

The mechanism of radial crack initiation and propagation due to rock blasting by explosives around a wellbore at a deep formation are studied analytically by a Green's function solution of the Lamé-Navier equation in elastodynamics. Then, the same problem is numerically simulated by FDM using FLAC2D, and by coupled FDM-DDM using FLAC2D-TDDQCR, respectively. The results are self-supporting and useful for understanding the mechanism of rock cracking around a borehole. The following main conclusions are gained through these analyses:

- The proposed analytical and numerical approaches can be well-used to simulate the radial crack propagation and to predict the crack patterns around the wellbore due to an explosion.
- It can verify the applicability of the explosion process for stimulating the wellbore and increasing productivity in an oil field.
- The resulting radial crack patterns and their lengths may be changed (increased or decreased) using stronger or weaker explosive materials based on project requirements and conditions.
- The explosion gas pressure can be numerically modeled to produce a hydraulic fracturing process of a horizontal wellbore driven in an unconventional hydrocarbon reservoir.

It should be noted that in this study only the major initiated radial cracks are considered in the cracks' propagation stage, whereas, the immature and smaller initiated dynamic cracks may increase the effect of the explosion in the dynamic fracturing which should be studied in future researches.

## 6. References

- [1] Gandossi, L., others and European Commission. Joint Research Centre. Institute for Energy and Transport. (2013) An overview of hydraulic fracturing and other formation stimulation technologies for shale gas production. Eur. Commission Jt. Res. Cent. Tech. Reports, Publications Office **26347**.
- [2] Peng, X., Cheng, Y., Xinyun, L., Zhang, X. and Libao, S. H. I. (2013) Explosive fracturing simulation experiment for low permeability reservoirs and fractal characteristics of cracks produced. *Pet. Explor. Dev.*, Elsevier **40**, 682–686.
- [3] Moridis, G. (2017) Literature review and analysis of waterless fracturing methods, California.
- [4] Lak, M., Fatehi Marji, M., Yarahamdi Bafghi, A. and Abdollahipour, A. (2018) Discrete element modeling of explosion-induced fracture extension in jointed rock masses. *J. Min. Environ.*, Shahrood University of Technology.
- [5] Liu, Z., Peng, S., Zhao, H., Geng, Y. and Zhang, Z. (2019) Numerical simulation of pulsed fracture in reservoir by using discretized virtual internal bond. *J. Pet. Sci. Eng.*, Elsevier **181**, 106197.
- [6] Brandon, C. W. (1962) Method of explosively fracturing a productive oil and gas formation, Google Patents.
- [7] Dysart, G. R., Spencer, A. M. and Anderson, A. L. (1969) Blast-fracturing, American Petroleum Institute.
- [8] Spencer, A. M., Dysart, G. R. and Anderson, A. L. (1970) New Blasting Methods Improve Oil Recovery. In *SPE Practical Aspects of Improved Recovery Techniques Symposium*, Society of Petroleum Engineers.
- [9] Laspe, C. G. and Roberts, L. N. (1971) A Mathematical Analysis of Oil and Gas Well Stimulation by Explosive Fracturing. In *SPE Rocky Mountain Regional Meeting*, Society of Petroleum Engineers.
- [10] Rogala, A., Krzysiek, J., Bernaciak, M. and Hupka, J. (2013) Non-aqueous fracturing technologies for shale gas recovery. *Physicochem. Probl. Miner. Process.* **49**.
- [11] Chen, Z., Yuan, Y., Yan, C., Wang, W. and Qin, Z. (2022) A Novel Carbon Dioxide Phase Transition Rock Breaking Technology: Theory and Application of Non-Explosive Blasting. *Processes*, MDPI **10**, 2434.
- [12] Agarwal, M. and Kudapa, V. K. (2022) Comparing the performance of supercritical CO<sub>2</sub> fracking with high energy gas fracking in unconventional shale. *MRS Energy Sustain.*, Springer **9**, 461–468.
- [13] Jiang, K., Deng, S., Jiang, X. and Li, H. (2023) Calculation of fracture number and length formed by methane deflagration fracturing technology. *Int. J. Impact Eng.*, Elsevier 104701.
- [14] Wang, J., Guo, T., Chen, M., Qu, Z., Liu, X. and Wang, X. (2023) Numerical simulation of deflagration fracturing in shale gas reservoirs considering the effect of stress wave impact and gas drive. *Int. J. Rock Mech. Min. Sci.*, Elsevier **170**, 105478.
- [15] Zhu, X., Feng, C. and Cheng, P. (2023) Improving

- reservoir permeability by electric pulse controllable shock wave. *J. Pet. Explor. Prod. Technol.*, Springer **13**, 1655–1667.
- [16] Goodarzi, M., Mohammadi, S. and Jafari, A. (2015) Numerical analysis of rock fracturing by gas pressure using the extended finite element method. *Pet. Sci.*, China University of Petroleum (Beijing) **12**, 304–315.
- [17] Guo, B., Shan, J. and Feng, Y. (2014) Productivity of blast-fractured wells in liquid-rich shale gas formations. *J. Nat. Gas Sci. Eng.*, Elsevier **18**, 360–367.
- [18] Shan, J. (2014) A Theoretical Investigation of Radial Lateral Wells with Shockwave Completion in Shale Gas Reservoirs. ProQuest Diss. Theses; Thesis (M.S.)--University Louisiana Lafayette, 2014.; Publ. Number AAT 1585873; ISBN 9781321655957; Source Masters Abstr. Int. Vol. 54-04.; 74 p.
- [19] Sheng, G., Su, Y., Wang, W., Zhang, Q. and Liu, J. (2015) Flow Behavior Analysis and Application of Complex-flow Model in Explosive Fracturing Well Using Fractal Theory. In SPE Middle East Oil & Gas Show and Conference, Society of Petroleum Engineers.
- [20] Settgaest, R. R., Vorobiev, O. Y., Morris, J. P., Herbold, E. B., Homel, M. A. and Annavarapu, C. (2017) Modeling of fracture opening by explosive products. In 51st US Rock Mechanics / Geomechanics Symposium 2017, American Rock Mechanics Association.
- [21] Shang, X., Zhang, Z., Yang, W., Wang, J. G. and Zhai, C. (2022) Fractal Analysis for Wave Propagation in Combustion--Explosion Fracturing Shale Reservoir. *Fractal Fract.*, MDPI **6**, 632.
- [22] Gong, D., Chen, J., Wang, W., Qu, G., Zhu, J., Wang, X. and Zhang, H. (2022) Numerical simulations of radial well assisted deflagration fracturing based on the smoothed particle hydrodynamics method. *Processes*, MDPI **10**, 2535.
- [23] Abdollahipour, A., Marji, M. F., Bafghi, A. Y. and Gholamnejad, J. (2016) Time-dependent crack propagation in a poroelastic medium using a fully coupled hydromechanical displacement discontinuity method. *Int. J. Fract.*, Springer **199**, 71–87.
- [24] Haeri, H., Marji, M. F. and Shahriar, K. (2015) Simulating the effect of disc erosion in TBM disc cutters by a semi-infinite DDM. *Arab. J. Geosci.*, Springer Berlin Heidelberg **8**, 3915–3927.
- [25] Marji, M. F. (2015) Simulation of crack coalescence mechanism underneath single and double disc cutters by higher order displacement discontinuity method. *J. Cent. South Univ.*, Central South University **22**, 1045–1054.
- [26] Hosseini\_Nasab, H. and Fatehi Marji, M. (2007) A semi-infinite higher-order displacement discontinuity method and its application to the quasistatic analysis of radial cracks produced by blasting. *J. Mech. Mater. Struct.*, Mathematical Sciences Publishers **2**, 439–458.
- [27] Haeri, H. (2015) Experimental crack analyses of concrete-like CSCBD specimens using a higher order DDM. *Comput. Concr. An Int. J.* **16**, 881–896.
- [28] Haeri, H., Shahriar, K., Marji, M. F. and Moarefvand, P. (2014) On the strength and crack propagation process of the pre-cracked rock-like specimens under uniaxial compression. *Strength Mater.*, Springer **46**, 140–152.
- [29] Rossmanith, H. P. (Ed.). (1983) *Rock Fracture Mechanics*, Springer Vienna, Vienna.
- [30] Whittaker, B. N., Singh, R. N. and Sun, G. (1992) *Rock fracture mechanics principles, design and applications, developments in geotechnical engineering*. Netherlands Elsevier Publ.
- [31] Marji, M. F. (2014) *Rock Fracture Mechanics with Displacement Discontinuity Method: Numerical Rock Fracture Mechanics, Higher Order Displacement Discontinuity Method, Crack Initiation and Propagation*, LAP LAMBERT Academic Publishing.
- [32] Dehghan Banadaki, M. M. and Mohanty, B. (2012) Numerical simulation of stress wave induced fractures in rock. *Int. J. Impact Eng.*, Pergamon **40–41**, 16–25.
- [33] Lak, M., Marji, M. F., Bafghi, A. Y. and Abdollahipour, A. (2019) Analytical and numerical modeling of rock blasting operations using a two-dimensional elasto-dynamic Green's function. *Int. J. Rock Mech. Min. Sci.*, Elsevier **114**, 208–217.
- [34] Omid Manesh, M., Sarfarazi, V., Babanouri, N. and Rezaei, A. (2023) Investigation of External Work, Fracture Energy, and Fracture Toughness of Oil Well Cement Sheath using HCCD Test and CSTBD Test. *J. Min. Environ.*, Shahrood University of Technology **14**, 619–634.
- [35] Bendezu, M., Romanel, C. and Roehl, D. (2017) Finite element analysis of blast-induced fracture propagation in hard rocks. *Comput. Struct.*, Pergamon **182**, 1–13.
- [36] Abdollahipour, A., Fatehi Marji, M., Yarahmadi Bafghi, A. and Gholamnejad, J. (2015) Simulating the propagation of hydraulic fractures from a circular wellbore using the Displacement Discontinuity Method. *Int. J. Rock Mech. Min. Sci.*, Pergamon **80**, 281–291.
- [37] Abdollahipour, A., Fatehi Marji, M., Yarahmadi-

- Bafghi, A. and Gholamnejad, J. (2016) Numerical investigation on the effect of crack geometrical parameters in hydraulic fracturing process of hydrocarbon reservoirs. *J. Min. Environ., Shahrood University of Technology* **7**, 205–214.
- [38 ] Abdollahipour, A., Fatehi Marji, M., Yarahmadi Bafghi, A. and Gholamnejad, J. (2016) DEM simulation of confining pressure effects on crack opening displacement in hydraulic fracturing. *Int. J. Min. Sci. Technol., Elsevier* **26**, 557–561.
- [39 ] Behnia, M., Goshtasbi, K., Marji, M. F. and Golshani, A. (2014) Numerical simulation of crack propagation in layered formations. *Arab. J. Geosci., Springer Berlin Heidelberg* **7**, 2729–2737.
- [40 ] Lak, M., Fatehi Marji, M., Yarahmadi Bafghi, A. R. and Abdollahipour, A. (2019) Discrete element modeling of explosion-induced fracture extension in jointed rock masses. *J. Min. Environ., Shahrood University of Technology* **10**, 125–138.
- [41 ] Hajibagherpour, A. R., Mansouri, H. and Bahaaddini, M. (2020) Numerical modeling of the fractured zones around a blasthole. *Comput. Geotech., Elsevier* **123**, 103535.
- [42 ] Tao, J., Yang, X.-G., Li, H.-T., Zhou, J.-W., Fan, G. and Lu, G.-D. (2020) Effects of in-situ stresses on dynamic rock responses under blast loading. *Mech. Mater., Elsevier* **145**, 103374.
- [43 ] Xie, L. X., Zhang, Q. B., Gu, J. C., Lu, W. B., Yang, S. Q., Jing, H. W. and Wang, Z. L. (2019) Damage evolution mechanism in production blasting excavation under different stress fields. *Simul. Model. Pract. Theory, Elsevier* **97**, 101969.
- [44 ] Hao, X., Du, W., Zhao, Y., Sun, Z., Zhang, Q., Wang, S. and Qiao, H. (2020) Dynamic tensile behaviour and crack propagation of coal under coupled static-dynamic loading. *Int. J. Min. Sci. Technol., Elsevier* **30**, 659–668.
- [45 ] Yang, L., Yang, A., Chen, S., Fang, S., Huang, C. and Xie, H. (2021) Model experimental study on the effects of in situ stresses on pre-splitting blasting damage and strain development. *Int. J. Rock Mech. Min. Sci., Elsevier* **138**, 104587.
- [46 ] Yang, R., Ding, C., Li, Y., Yang, L. and Zhao, Y. (2019) Crack propagation behavior in slit charge blasting under high static stress conditions. *Int. J. Rock Mech. Min. Sci., Elsevier* **119**, 117–123.
- [47 ] Lak, M., Fatehi Marji, M. and Yarahmadi Bafghi, A. (2018) A finite difference modelling of crack initiation in rock blasting. In *The 2018 World Congress on Advances in Civil, Environmental, & Materials Research (ACEM18)*, Songdo Convensia, Incheon, Korea.
- [48 ] Changyou, L., Jingxuan, Y. and Bin, Y. (2017) Rock-breaking mechanism and experimental analysis of confined blasting of borehole surrounding rock. *Int. J. Min. Sci. Technol., Elsevier* **27**, 795–801.
- [49 ] Lak, M., Fatehi Marji, M., Yarahmadi Bafghi, A., Abdollahipour, A. and Pourghasemi Sagand, M. (2023) Analytical solution of the explosion-induced wave propagation in rock using elastodynamic theory. *J. Anal. Numer. Methods Min. Eng., Yazd University* **13**, 57–65.
- [50 ] Sadd, M. H. (2009) *Elasticity: theory, applications, and numerics*, Academic Press.
- [51 ] Sanei, M., Duran, O., Devloo, P. R. B. and Santos, E. S. R. (2020) An innovative procedure to improve integration algorithm for modified Cam-Clay plasticity model. *Comput. Geotech., Elsevier* **124**, 103604.
- [52 ] Sanei, M., Devloo, P. R. B., Forti, T. L. D., Durán, O. and Santos, E. S. R. (2022) An innovative scheme to make an initial guess for iterative optimization methods to calibrate material parameters of strain-hardening elastoplastic models. *Rock Mech. Rock Eng., Springer* 1–23.
- [53 ] Duran, O., Sanei, M., Devloo, P. R. B. and Santos, E. S. R. (2020) An enhanced sequential fully implicit scheme for reservoir geomechanics. *Comput. Geosci., Springer* **24**, 1557–1587.
- [54 ] Sanei, M., Duran, O., Devloo, P. R. B. and Santos, E. S. R. (2021) Analysis of pore collapse and shear-enhanced compaction in hydrocarbon reservoirs using coupled poro-elastoplasticity and permeability. *Arab. J. Geosci., Springer* **14**, 1–18.
- [55 ] Sanei, M., Duran, O., Devloo, P. R. B. and Santos, E. S. R. (2022) Evaluation of the impact of strain-dependent permeability on reservoir productivity using iterative coupled reservoir geomechanical modeling. *Geomech. Geophys. Geo-Energy Geo-Resources, Springer* **8**, 54.
- [56 ] Trivino, L. F. and Mohanty, B. (2015) Assessment of crack initiation and propagation in rock from explosion-induced stress waves and gas expansion by cross-hole seismometry and FEM–DEM method. *Int. J. Rock Mech. Min. Sci., Elsevier* **77**, 287–299.
- [57 ] Wilmott, P., Howison, S. and Dewynne, J. (1995) *The mathematics of financial derivatives: a student introduction*, Cambridge university press.
- [58 ] Chaudhry, M. H. (2008) *Open-channel flow: Second Edition*. Open-Channel Flow Second Ed., Springer US 1–523.
- [59 ] Crouch, S. L. (1976) Solution of plane elasticity problems by the displacement discontinuity method. I. Infinite body solution. *Int. J. Numer. Methods Eng.,*

- Wiley-Blackwell **10**, 301–343.
- [60 ] Crouch, S. L., Starfield, A. M. and Rizzo, F. J. (1983) Boundary Element Methods in Solid Mechanics. *J. Appl. Mech.* **50**, 704.
- [61 ] Shou, K. J. and Crouch, S. L. (1995) A higher order displacement discontinuity method for analysis of crack problems. *Int. J. Rock Mech. Min. Sci., Pergamon* **32**, 49–55.
- [62 ] Marji, M. F., Hosseini-Nasab, H. and Kohsary, A. H. (2006) On the uses of special crack tip elements in numerical rock fracture mechanics. *Int. J. Solids Struct., Pergamon* **43**, 1669–1692.
- [63] Marji, M. F. (2013) On the use of power series solution method in the crack analysis of brittle materials by indirect boundary element method. *Eng. Fract. Mech., Pergamon* **98**, 365–382.
- [64] Manual, F. U. (2016) Version 8.0, Itasca Consulting Group. Inc., Minneapolis, Minn.
- [65 ] Lysmer, J. and Kuhlemeyer, R. L. (1969) Finite dynamic model for infinite media. *J. Eng. Mech. Div., ASCE* **95**, 859–878.
- [66 ] Lak, M., Baghbanan, A. and Hashemolhoseini, H. (2017) Effect of seismic waves on the hydro-mechanical properties of fractured rock masses. *Earthq. Eng. Eng. Vib.* **16**, 525–536.
- [67 ] Yousefian, H., Soltanian, H., Marji, M. F., Abdollahipour, A. and Pourmazaheri, Y. (2018) Numerical simulation of a wellbore stability in an Iranian oilfield utilizing core data. *J. Pet. Sci. Eng., Elsevier* **168**, 577–592.
- [68 ] Lak, M., Fatehi Marji, M., Yarahamdi Bafghi, A. and Abdollahipour, A. (2018, July) Numerical Modelling of Crack Initiation around a Wellbore Due to Explosion. *Int. J. Environ. Chem. Ecol. Geol. Geophys. Eng.*
- [69 ] Bhandari, S. (1997) *Engineering Rock Blasting Operations*, Taylor & Francis.
- [70] Jimeno, E. L., Jimino, C. L. and Carcedo, A. (1995) *Drilling and Blasting of Rocks*, Taylor & Francis.
- [71 ] Cho, S. H. and Kaneko, K. (2004) Influence of the applied pressure waveform on the dynamic fracture processes in rock. *Int. J. Rock Mech. Min. Sci., Elsevier* **41**, 771–784.
- [72 ] Chun-ruì, L., Li-jun, K., Qing-xing, Q., De-bing, M., Quan-ming, L. and Gang, X. (2009) The numerical analysis of borehole blasting and application in coal mine roof-weaken. *Procedia Earth Planet. Sci., Elsevier* **1**, 451–459.
- [73 ] Duvall, W. (1953) STRAIN-WAVE SHAPES IN ROCK NEAR EXPLOSIONS. *GEOPHYSICS, Society of Exploration Geophysicists* **18**, 310–323.
- [74 ] Sharpe, J. A. (1942) THE PRODUCTION OF ELASTIC WAVES BY EXPLOSION PRESSURES. I. THEORY AND EMPIRICAL FIELD OBSERVATIONS. *GEOPHYSICS, Society of Exploration Geophysicists* **7**, 144–154.
- [75] Gokhale, B. V. (2011) *Rotary Drilling and Blasting in Large Surface Mines*. CRC Press, CRC Press.
- [76 ] Moradi, A., Tokhmechi, B., Rasouli, V. and Fatehi Marji, M. (2017) A comprehensive numerical study of hydraulic fracturing process and its affecting parameters. *Geotech. Geol. Eng., Springer* **35**, 1035–1050.
- [77] Abdollahipour, A. and Marji, M. F. (2020) A thermo-hydromechanical displacement discontinuity method to model fractures in high-pressure, high-temperature environments. *Renew. Energy, Elsevier* **153**, 1488–1503.
- [78] Wapenaar, K. (2017) A single-sided representation for the homogeneous Green's function of a unified scalar wave equation. *J. Acoust. Soc. Am., Acoustical Society of America* **141**, 4466–4479.